Inferring Reservoir Operating Pattern via Residence Time across the Mekong Basin using only Space Observations

Matthew Bonnema and Faisal Hossain

Department of Civil and Environmental Engineering, University of Washington

More Hall 201, Seattle, WA 98195, USA

Submitted to:
Water Resources Research

Corresponding Author
Faisal Hossain
Department of Civil and Environmental Engineering
University of Washington, Seattle, WA 98195
Email: fhossain@uw.edu

Abstract

This study explores the operating pattern of artificial reservoirs using residence time and a purely satellite based technique for the Mekong Basin. Overall residence times of individual reservoirs ranged from 0.09 years to 4.04 years. The current set of reservoirs appears to have increased the residence time of the entire Mekong basin by about 1 month. However, if sub-basin variability is considered, the satellite-based method depicts a different picture. Residence time increases to 4 months when only regulated flows are considered. If low residence time reservoirs on major rivers are excluded and reservoirs on higher stream-order rivers considered, residence time increases to 1.3 years. Overall three strong patterns at the intersection of hydrology and human regulation of flow appear in this study. First, Mekong reservoirs experience higher residence time in the dry season and lower residence time in the wet season. Second, higher precipitation generally leads to lower residence time, while lower precipitation leads to higher residence time. Third, reservoirs on higher ordered streams tend to have lower residence time which also appears to be the global trend according to a set of more than 6000 reservoirs. The take-home message of this study is that satellite observations, in combination with physical models forced with satellite data can elucidate the spatio-temporal variability of reservoir behavior that is fundamentally impossible to derive in ungauged basins of the developing world. We demonstrate in this study that the requirement for ground data to monitor current or historical behavior of dams is not necessary.

Key words: Reservoirs, residence times, Mekong, satellites

1. Introduction

Man-made reservoirs and dams provide tremendous societal benefits in the form of hydropower generation, flood control, irrigation, and water supply. However, by altering river flows and limiting transport of sediments, nutrients, and biota, these dams cause ecologically damaging impacts on the natural river system (Ligon et al. 1995). One study concluded that 25%-30% of global sediment discharge is trapped within reservoirs annually (Vörösmarty et al. 2003). Numerous other studies have established links between dams and negative effects on the downstream ecosystem (Pringle 2003; Graf 2006). One key parameter for understanding these impacts is reservoir residence time.

Residence time, as defined in Monsen et al. (2002), is "*how long a parcel, starting from a specified location within a waterbody, will remain in the waterbody*". For reservoirs, the specified starting location is typically the point in which water enters the reservoir from upstream. The residence time of a reservoir controls biochemical processes such as nutrient accumulation and eutrophication processes (Ambrosetti et al. 2003) as well as sedimentation (Kummu et al. 2010) and fish population dynamics (Beamesderfer et al. 1990). The residence time of a reservoir can be used to obtain first order approximations of these and other complex processes, which dictate the impact the reservoir has on the river system. In short, time varying residence time can be considered as a 'wholesale' metric that can capture not only a reservoir's operating pattern, but also its overall character and its multi-faceted impact on hydrology, geomorphology and ecosystem function.

Past studies have characterized reservoir residence time as the volume of the reservoir divided by the mean annual inflow (Vörösmarty et al. 1997; Kummu et al. 2010, Lehner et al. 2011), which is more indicative of the design feature of a dam. This method also makes the

assumption of steady state conditions within the reservoirs, where volume remains constant and inflow is equal to outflow. This may be valid when studying long time scales, where annual inflow and outflow are equal. However, residence time can fluctuate greatly at shorter time scales due to variations in inflow, outflow, volume changes and mixing processes (Rueda et al. 2006). Accounting for this temporal variability in reservoirs requires observing these time varying parameters.

Unfortunately, in-situ observations are largely unavailable, primarily in developing regions due to the inability of agencies to make observations or the unwillingness of agencies to provide their data to the public for political or security reasons. Such a situation has led many traditional water managers to believe that reservoir behavior cannot be elucidated to the level required for making decisions without actual in-situ monitoring. This issue is made more urgent by the fact that dam construction in such regions is increasing (Zarfl et al. 2015). With thousands of new dams planned for construction, it is imperative that the impacts of dams in these regions be more closely studied with or without in-situ data. The situation pertinent to lack of in-situ data is likely to persist or only worsen in future (Gebregiorgis and Hossain 2014). Thus, observations from space (i.e. satellite data) are the only viable alternative. Satellite remote sensing has been shown to have remarkable utility in the field of reservoir studies (Gao et al. 2012; McGuire et al. 2006; Allee and Johnson 1999; Crétaux and Birkett 2006). Remotely sensed geophysical variables have the potential to provide the information necessary to estimate reservoir residence time in a more rigorous way.

Bonnema et al. (2016) used a combination of radar altimetry and Shuttle Radar and Topography Mission (SRTM) data to estimate the outflow of a reservoir in Bangladesh, which showed promise in providing the storage changes and outflows of reservoirs in ungauged basins.

Furthermore, numerous studies also suggest that visible imaging missions such as Landsat can provide reasonable estimates of reservoir surface area (Gao et al. 2015, Ji et al. 2009, Seeber et al. 2010). As we will show in this study, reservoir surface area is a key ingredient for deriving reservoir volume and as a result, residence time.

One region of particular interest in this paper is the Mekong River Basin (MRB). The Mekong Basin is relatively underdeveloped in terms of river impoundments (Kummu and Sarkula 2008). There are currently 30 dams in the basin, three of which are located on the main stem of the Mekong River in China (Keskinin et al. 2012). As of 2012, there were 14 dams currently under construction, with another 78 planned (Keskinin et al. 2012). Sixty million people live in the Lower Mekong Basin alone, and 80% rely directly on the river for their food supply, primarily fish and floodplain agriculture. A Mekong River Commission (MRC) report finds that the planned main stem dams would inflict USD 476 million/year of damages on fisheries within the river system, excluding any impacts on delta and costal fisheries (International Center for Environmental Management 2010). Furthermore, these same dams are predicted to cause USD 25.1 million/year in lost agricultural land and USD 24 million/year in reduced nutrient loading to floodplain agriculture (International Center for Environmental Management 2010). Understanding the impacts of these dams in greater detail is essential and begins with understanding the dams that currently exist in the basin. Residence time is a wholesale and convenient metric in quantifying the multi-faceted effects and operating pattern of a reservoir. Thus, the objective of this study is to estimate the residence time of current reservoirs in the MRB and its temporal variation.

Such a study can provide the foundation for studying reservoirs in other developing basins undergoing rapid change due to dam construction such as the Irrawaddy, Yangtze, or

Zambesi. The benefit of a satellite based approach is that it is unhindered by lack of availability of in-situ data and has global applicability. Satellite-based reservoir technique can therefore be scaled regionally or globally to answer for diverse set of stakeholders and scientific communities fundamental questions that have not been answered before. Some of these questions are: *How has the residence time of surface water changed due to water management and what are its implications for ecosystem services and flood risk in river basins? How is residence time of managed water in regulated river systems likely to change in the future due to climate change, increasing development pressures and aggressive dam building plans by the developing world?*

In the text that follows, section 2 describes the reservoirs studied here and provides an outline of the data available. Section 3 provides an overview of the method used to calculate residence time. Section 4 shows the results and provides discussion. Section 5 concludes with an overview and direction for future study.

2. Study Region

The MRB encompasses an area of 795,000 km^2 and spans six nations of China, Myanmar, Laos, Thailand, Cambodia, and Vietnam. It has an average annual discharge of 457 km^3. The basin experiences a tropical monsoon climate where a majority of the precipitation arrives from May through October, resulting in a similar seasonal pattern in streamflow. This study focused on the 20 large reservoirs identified by the Global Reservoir and Dam (GRanD) Database (Lehner et al. 2011). Figure 1 shows a map of the Mekong Basin with these 20 dams as well as future planned or under construction dams identified by Zarfl et al. 2015.

Table 1 lists the dam/reservoir name and identification number along with their capacity and degree of regulation (capacity divided by annual inflow), taken from the GRanD Database.

The capacity of these reservoirs ranges from 22.8 million m^3 to 7030 million m^3 with an average of 961 million m^3. Degree of regulation (DOR) is the reservoir capacity expressed as a percentage of the mean annual inflow into the reservoir, which can be assumed as the 'design' residence time of the reservoir.

For validation of the satellite-based technique, daily time series of in-situ reservoir water levels was acquired for specific reservoir sites via our institutional agreement with various nations of the MRB (e.g. Vietnam). In other cases, daily time series of reservoir volumes of some reservoir sites was acquired from publicly available websites (e.g. Thaiwater.net). This is outlined in greater detail in Section 3.

3. Methodology

3.1 Residence Time

The key ingredients for estimating residence time are inflow (I), storage (S), and outflow (O). The driving concept behind the residence time calculation is that these terms obey a mass balance for every reservoir, given by Equation 1, where I is inflow, O is outflow, and ΔS is the change in storage over a duration of time.

$$O = I - \Delta S \tag{1}$$

With the water in reservoirs obeying mass balance, several basic assumptions can be made in order to simplify the calculation of reservoir residence time:

1. A water parcel which enter the reservoir over a specific duration does not mix with other water parcels within the reservoir.
2. Water parcels exit the reservoir in order from oldest to newest.

With these two assumptions, the length of time a parcel of water spends in the reservoir can be identified. Generally speaking, a monthly time step was used, so the residence time of the inflow entering a reservoir during one month is the amount of time until all of the water is released that was in the reservoir just after the monthly inflow parcel arrived. This is expressed by Equation 2, where t_0 denotes the time step of interest, $\theta(t_0)$ is the residence time of the water entering the reservoir at time t_0, and t_R is the time step in which the water that entered at time t_0 is released from the reservoir. This time of release is calculated by summing the amount of water exiting the reservoir in each time step, O(t), beginning at t_0 and ending when the sum is equal to the volume of the reservoir, $V(t_0)$ plus the amount of inflow, $I(t_0)$, at the time step of interest, t_0.

$$\begin{aligned} \theta(t_0) &= t_R - t_0 \\ I(t_0) + V(t_0) &= \sum_{t}^{t_R} O(t) \end{aligned} \tag{2}$$

To average residence time across time or to average residence time between multiple reservoirs, an inflow weighted approach was used, as shown in Equation 3.

$$\theta_{avg} = \sum_{i=1}^{n} \frac{I_i \theta_i}{I_{avg}} \tag{3}$$

Where θ_{avg} is the residence time averaged over some period of time or space, θ_i and I_i are the residence time and inflow, respectively, of time period or reservoir i, and I_{avg} is the average inflow of the reservoir.

3.2 Reservoir Inflow

In order to estimate the inflow into each reservoir, a 0.1 degree resolution Variable Infiltration Capacity (VIC) Model of the MRB was employed (Liang et al.1994). The model was constructed using land cover data from the Global Land Cover Characterization (GLCC) dataset and soil data prepared by the Harmonized World Soil Database (HWSD) (Loveland et al. 2000;

FAO, 2012). Monthly leaf area index and albedo were provided by the Moderate Resolution Imaging Spectroradiometer (MODIS) mission and topography information was obtained from SRTM. This model was run at the daily time step from 2002 through 2015 (14 years), providing surface water fluxes for each 0.1 degree grid cell. The meteorological forcings such temperature (minimum and maximum), wind speed and precipitation were obtained from 237 weather station records archived as Global Summary of the Day (GSOD) by National Climatic Data Center (NCDC). These modeled fluxes were then re-gridded to 0.01 degree resolution and run through a streamflow routing model of the basin to obtain daily inflow into each reservoir (Lohmann et al. 1996). The re-gridding was necessary to simulate reservoir inflow at the appropriate resolution because some of the reservoirs are built on smaller rivers that would not appear in 0.1 degree resolution topography. The routing model used estimates of surface runoff from the VIC model and routed this water to river channels according to input topographical information. The daily flows were then aggregated into average monthly inflow. Figure 2 shows monthly averaged basin precipitation and basin outflow at the MRB delta (i.e. the basin outlet), averaged across the entire 2002 through 2015 time period. Precipitation and outflow are both seen to increase from May through September, decrease from September through December, and then remain stably low from January through April. This pattern is fairly representative of the local inflow behavior at each reservoir. Figure 3 shows the annual average basin precipitation and basin outflow from 2002 through 2015. A point to note is that the VIC model represents natural stream flows and does not take the effects of reservoir operations into account. Therefore, the inflow of reservoirs downstream of other reservoirs was adjusted according the outflow of each upstream reservoir (discussed in greater detail in Section 3.4).

3.3 Reservoir Storage

The estimation of reservoir storage was a three step process. First, a relationship between reservoir surface area and elevation was established for each reservoir. This relationship is known as the area-elevation curve. Next, the area-elevation curve was used to convert satellite measurements of either water surface elevation or surface area into reservoir volume (known as the area-volume curve). Finally, a monthly operations curve was established from a long record of satellite observations and used to fill gaps in the satellite record. Each of these processes are described in greater detail below.

3.3.1 Area-Elevation Curve

The method used here is similar to the method employed in Bonnema et al. (2016). For each reservoir, a 30 m resolution digital elevation model (DEM) provided by the Shuttle Radar and Topography Mission (SRTM) was classified into 1 m elevation bands over the reservoir and surrounding area. The surface area of each band provides an estimate of the reservoir surface when water reaches that elevation. This provided information on the bathymetry of the reservoir above the elevation of the water at the time of the SRTM observation (i.e., February 2000). To estimate the bathymetry below this elevation, a power curve was fitted to the lowest observed elevation bands and extended below the water surface. This curve is used to extrapolate the curve to capture the bathymetry below the level the water was at when SRTM observed the reservoir.

3.3.2 Reservoir Volume

The volume of a reservoir is then computed using either radar altimetry based water surface elevations or spectral (visible) band based water surface area from Landsat. The

Sirindhorn Reservoir is the only reservoir of the 20 examined here that is observed by a satellite altimeter. For this reservoir, elevations obtained from the Jason-2 satellite altimetry mission were used. Using the area-elevation curve, the reservoir surface area corresponding to the observed elevation was identified. For all other reservoirs, Landsat images were used to estimate reservoir surface area. Specifically, the normalized difference water index (NDWI) was used to classify water pixels from 30 m resolution Landsat spectral images (McFeeters 1996). This method identifies which pixels of a Landsat image likely contain water by calculating the NDWI for each pixel, according to Equation 4:

$$NDWI = \frac{X_{green} - X_{nir}}{X_{green} + X_{nir}} \tag{4}$$

Where X_{green} and X_{nir} are the reflectance values in the green and near infrared wavelengths, respectively. The green wavelength corresponds to Band 3 from Landsat 8 and Band 2 from Landsat 4,5, and 7. The near infrared wavelength corresponds to Band 5 from Landsat 8 and Band 4 from Landsat 4,5, and 7. Pixels with NDWI greater than 0 were classified as water pixels and pixels with NDWI less than 0 were assumed to not contain surface water. The surface area of the water pixels is then the estimate of the reservoir surface area at the time of the Landsat overpass. Again, using the area-elevation curve, the corresponding water surface elevation was identified.

With both water elevation and surface area known, the volume of the reservoir can be computed by estimating the volume of water required to fill the reservoir to the storage capacity listed in the GRanD Database (Gao et al. 2012). This is done using a trapezoidal approximation (Equation 5), where V is the volume of the reservoir, A is the reservoir surface area, h is the reservoir elevation and the subscript c denotes these quantities at reservoir capacity.

$$V = V_c - (A_c + A)(h_c - h)/2 \quad (5)$$

3.3.3 Reservoir Operations Curve

A significant issue with building a time series of reservoir surface areas with Landsat images is the potential for unusable images due to cloud cover, which can lead to long temporal gaps in data. This was overcome here by employing a method similar to the approach outlined in Yoon and Beighley (2014). Here, the assumption is made that reservoirs are operated at a relatively stable level on a sub monthly scale and when looked over a long record, variability of reservoir operation at sub-monthly scales remains within a narrow range. This is a fairly realistic assumption as most reservoirs strive to follow the rule curve and make release and storage decisions according to a pre-defined standard operating procedure (SOP).

The reservoir volumes estimated from the entire record of Landsat images were thus grouped by month and the average reservoir volume for each month is calculated. This formed an approximation of the reservoir operations curve. This process is illustrated by Figure 4. The utilization of green and NIR Landsat bands to estimate water surface is depicted in the upper panels and the derivation of the area-elevation curve is shown in the lower left panel. A single water surface area estimate, when paired with the area-elevation curve, led to a single point on the operations curve in the lower right panel. With a long record of Landsat images, the average reservoir volume for each month can be estimated. This monthly average is the approximation of the operations curve, which was then used to fill gaps in the time series of reservoir volume generated from Landsat images. For each monthly time step where no cloudless Landsat image exists, reservoir volume from the approximated operations curve was used. Figure 5 shows the fraction of months without any usable Landsat images from 2002 through 2015, averaged across all reservoirs, as well as the range of unobserved months of all reservoirs. Unsurprisingly, the

months with the least amount of usable Landsat images occur when precipitation is the highest (see Figure 2).

3.4 Reservoir Outflow

Reservoir outflow was estimated using the same mass balance described earlier by Equation 1 (Bonnema et al. 2016). This method has been shown to provide accurate reservoir outflow estimates at monthly time scales for the Kaptai Reservoir in Bangladesh, which is located in a similar tropical monsoon climate as the MRB (Bonnema et al. 2016). Based on the results of this past study, evaporation was neglected from the mass balance.

As previously stated, these outflows were used to correct the inflows of downstream reservoirs. Since the routing model conserves water in the river network, the downstream inflows are adjusted by the amount of total storage change in upstream reservoirs (Equation 5) where I_{adj} is the adjusted inflow, I is the natural inflow (modeled by VIC), and ΔS_{up} is the storage change of upstream reservoirs.

$$I_{adj} = I - \sum \Delta S_{up} \tag{5}$$

4. Results and Discussion

4.1 Validation of Satellite Based Volume Estimates

Figure 6 plots ground observed (in-situ) volume of the Sirindhorn Reservoir alongside estimated reservoir volume. Comparison between these two volumes and taking the ground observed value as the true volume results in a root mean squared error (RMSE) of 0.27 km^3, which is 19% of the average reservoir volume in this time period. This indicates that the altimetry based method of estimating reservoir volume is successful (within a 20% error range)

in capturing the month-to-month reservoir volume fluctuations. Unfortunately, the Sirindhorn Reservoir is the only reservoir studied here that was overpassed by a satellite altimeter to provide skillful height variations. Nevertheless, the close agreement between satellite-based volume and the in-situ volume established a good level of trustworthiness in our comprehensive satellite-based approach that synthesizes multiple platforms for other reservoirs of the MRB. Figure 7 compares the actual monthly water level elevations of the Yali Reservoir to elevations derived from the visible Landsat images. This Landsat derived water surface elevations exhibit an RMSE of 0.57 m, which is 8.6% of the range in actual water surface elevations observed during this time period. Overall, these results signify that both the Landsat based method and the altimeter-based method are certainly capable of accurately estimating water surface heights and consequential volume changes.

4.2 Reservoir Residence Time

Figure 8 displays how the resulting residence times are distributed throughout the MRB. These residence time values are also shown in Table 2 broken down as a function of season: wet season (June through October) and the dry season (November through May). Residence times ranged from 0.09 years to 4.04 years. Figure 9 shows the estimated residence operations curves, each normalized by their maximum storage so that they can be plotted together. While there is variation among the different reservoirs, there is a clear trend of higher volume at the beginning of the dry season, followed by decline into the wet season. At the end of the wet season, the reservoirs fill again. This trend is highlighted by the average normalized operations curve which is shown in black.

Figure 10 shows a comparison between the residence time estimated in this study and the DOR estimated in the GRanD Database. DOR was estimated in Lehner et al. 2011 by dividing reservoir capacity by long term average annual inflow. DOR is essentially the reservoir capacity expressed as a percentage of the annual average inflow, and is similar to residence time, as calculated using a similar method than the one employed here. Thus, it is a good point of comparison for the resulting residence times from this study. Figure 10 presents DOR as the number of years of inflow which can be stored within a reservoir. This figure shows some agreement between the simple to obtain DOR and the temporally varying approach employed here, however other reservoirs show significant differences. No correlation between the capacity, stream order, or reservoir use could be established that would explain this difference, although a larger sample size of reservoirs could provide greater clarity.

4.2.1 Temporal Variations

As seen in Table 2, residence time was typically larger during dry season than wet season. This agrees with what is known about seasonal variations in stream flow and reservoir operations. Figure 9 clearly illustrates the typical seasonal trend observed in reservoir volume, where reservoirs are kept low during the start of the wet season and allowed to fill towards the end of the wet season. This is followed by high reservoir volume in the beginning of the dry season, as reservoirs are then being used to store water and release it in a controlled fashion throughout the wet season. The low inflows in the dry season led to a decrease as water is discharged for irrigation, water supply or hydropower generation. It is this long, slow release of water in the dry season that causes residence time to increase. Similarly, the rapid outflows and lower volume combined in the wet season lead to lower residence time. Figure 11 plots the

average monthly residence time of all reservoirs, each normalized by the reservoir's average residence time. This plot further elucidates the seasonal trend in residence time.

It also reveals that reservoirs with higher residence time exhibit less seasonal fluctuation in residence time (reservoirs with residence time greater than 1 year are shown in red in Figure 11). Similarly, reservoirs with lower residence time have more pronounced seasonal variations than reservoirs with higher residence time. A likely explanation for this pattern is that reservoirs with higher residence time tend to have higher storage capacity relative to their inflow. This indicates that such reservoirs would be inherently less sensitive to fluctuations in inflow, resulting in a more consistent residence time. For example, water entering the Houayho Reservoir is estimated to stay within the reservoir for approximately 4 years before being released. This water resides in the reservoir over the course of multiple wet and dry seasons, dampening the seasonal trend described earlier.

Figure 12 shows the yearly average residence time for each reservoir from 2002 through 2015. Note that since the method employed here estimates residence time by following a parcel of water from reservoir entry to exit, it is incapable of estimating residence time of parcels which do not exit reservoirs within the time period. For this reason, reservoirs with higher residence time do not have residence time estimates for the entire time period. While there are some variations among the reservoirs, there are also clear trends. Most reservoirs experience rises in residence time in 2009, 2012, and 2014. Normalizing theses residence times by reservoir averages, averaging across all reservoirs, and plotting with precipitation reveals a possible source of these yearly fluctuations. Figure 13 shows a negative relationship between average annual precipitation and basin averaged residence time, where residence time increases when precipitation decreases. Similarly, residence time decreases when precipitation is higher. This

trend is made evident by a correlation coefficient of -0.65 between annual average precipitation and annual basin averaged residence time. Logically, when there is more water in the river system, reservoirs typically have higher releases, which leads to lower residence time. Conversely, when there is less water in the river system, inflows and outflows are lower, leading to higher residence time. Additionally, in dryer time periods, reservoirs may be operated in such a way to withhold more water than usual to provide additional security in water supply for the uncertain future.

4.2.2 Spatial Variations

Figure 8 qualitatively suggests that reservoir residence time is equally distributed across the basin and there appears to be no correlation between reservoir location and residence time. While this may be the case, the location of the reservoir within the river network plays an important role in the overall effect of the reservoir on basin residence time. Considering the Mekong basin as a whole, the reservoirs studied here caused an average increase in the length of time water spends in the river network by only 3 weeks (0.059 years). When considering only the portion of the overall flow that is regulated by these reservoirs (totaling 17% of basin runoff), the average increase in residence time rises to just over 4 months (0.35 years). Most of the regulated discharge passes through two reservoirs, the Manwan Reservoir on the main stem of the Mekong in China and the Pak Mun Reservoir on the Mun River, a major tributary of the Mekong in Thailand. While neither of these reservoirs are particularly small, they both experience significantly large flows, leading to the extremely short residence times observed in this study. Because of their low residence times, their impact on the overall residence time of the basin is limited. If these dams are excluded, and only regulated discharge from higher order rivers is

considered, the average increase in residence of this discharge becomes 1.3 years. This flow only makes up 3.5% of the total basin discharge, so while these reservoirs have little impact on the basin as a whole, they do have significant impact on local hydrology, specifically, on lower order streams within the river network.

The role of stream order is further explored in Figure 14, where residence time is plotted against stream order for the Mekong reservoirs studied here, as well as for all reservoirs in the GRanD Database and the average of each stream order. GRanD Database reservoir residence time was taken as their DOR expressed in years. Note that there are some reservoirs in the GranD database with residence times higher than 10 years. These were excluded from the plot so that the Mekong reservoirs could be compared with the global situation in better detail. The averages shown include reservoirs beyond the extent of the plot. There is a clear negative trend between residence time and stream order in the global set of reservoirs from GranD, which appears to be mirrored in the Mekong reservoirs. This trend suggests that the most impactful reservoirs in terms of residence time increase, tend to be built on lower order rivers. However, higher order reservoirs impact a larger amount of flow. As stream order increases, so does river flow and it becomes increasingly difficult or infeasible to build a reservoir that retains water for long periods of time under such high flows. Greater control of smaller flows in lower order streams can be imposed by smaller reservoirs that can be more feasible to build.

5. Conclusion

Three strong patterns in residence time of reservoirs in the MRB emerge from this study. Reservoirs experience higher residence time in the dry season and lower residence time in the wet season, with this trend being less prominent in reservoirs with longer residence times. This is

an intuitive trend one would expect in a river basin dominated by strongly seasonal hydrology (such as the Monsoon). However, the fact that satellite observations and physical hydrological model alone are able to elucidate such a trend without any help from in-situ observations is notable for ungauged and developing river basins. Additionally, reservoirs in the MRB experience yearly fluctuations in residence time in parallel with fluctuations in precipitation. Specifically, higher precipitation leads to lower residence time, while lower precipitation leads to higher residence time. This pattern highlights the connectivity of the reservoir operations to the water inputs into the river system. Furthermore, the current reservoirs collectively have insignificant impact on the overall MRB system if the MRB is assumed as one single control volume. However, there are two caveats to this 'systems' approach. First – the systems approach of a single residence time for the entire basin is valuable for water balance studies only when all riparian nations are working together on a shared vision for integrated water resources management. Secondly – the single basin-wide metric does not paint the real picture of spatially and temporally diverse human impacts of reservoirs within a basin to identify appropriate and local water management strategies. For example, many reservoirs on lower stream-order rivers have significant impact on the localized streamflow. Lastly – the future plans for MRB development involves the building of three times more the current number of basins that certainly informs us that even the basin-wide impact on residence time will no longer remain insignificant.

The identification of these spatial and temporal trends in reservoir residence time indicate that it is feasible to estimate residence time using the primarily satellite observation based method applied here. This is perhaps the key take home message of our study – that satellites can indeed pick out the diverse variability of residence time due to reservoir construction in

ungauged and international river basins that is otherwise intractable. As satellite observations of the water cycle (surface water inundation, height; Biancamaria et al., 2016), precipitation, soil moisture become increasingly more widespread in the near future, it appears that the scientific community will be able to rely on space observations to understand the potential impact of reservoir development planned by each riparian nation. The hope is that the availability of such understanding across a basin will counter the secrecy that is typically adopted by each riparian nation of international river basins, and result in a more cooperative environment where nations will work together for the benefit of all the stakeholders of the basin.

[**Acknowledgements:** The authors gratefully express the in-situ data obtained from Mr. Duc Long of Vietnam National Center for Hydrometeorological Forecasting, Hanoi. Such data were obtained as part of a USAID PEER (Program for Enhanced Engagement in Research) program maintained by the second author with Vietnamese water agencies. This work was partially supported by NASA Applied Sciences Grant NNX 15 AC63G under the Water Resources Program and NASA SWOT Science Team Grant NNX16AQ54G_9-15-16. Lastly, the authors gratefully acknowledge the guidance received from Dr. Hyongki Lee of University of Houston on the use of satellite altimeter data.]

6. References

Allee, R. J., and J.E. Johnson (1999), Use of satellite imagery to estimate surface chlorophyll a and Secchi disc depth of Bull Shoals Reservoir, Arkansas, USA. International Journal of Remote Sensing, 20(6), 1057-1072.

Ambrosetti, L. Barbanti, N. Sala (2003), Residence time and physical processes in lakes J. Limnol., 62, pp. 1–15

Beamesderfer and C. Raymond, et al. (1990), Management implications of a model of predation by a resident fish on juvenile salmonids migrating through a Columbia River reservoir. *North American Journal of Fisheries Management*, 10(3), pp. 290-304.

Biancamaria, S., D. P. Lettenmaier and T. Pavelsky (2016), The SWOT Mission and Its Capabilities for Land Hydrology, Surveys of Geophysics, 37(2), pp. 307-337.

Bonnema, M., S. Sikder, Y. Miao, X. Chen, F. Hossain, I. Ara Pervin, S. M. Mahbubur Rahman, and H. Lee (2016), Understanding satellite-based monthly-to-seasonal reservoir outflow estimation as a function of hydrologic controls, Water Resour. Res., 52, 4095–4115, doi:10.1002/2015WR017830.

Crétaux, J. F., and C. Birkett, (2006). Lake studies from satellite radar altimetry. Comptes Rendus Geoscience, 338(14), pp. 1098-1112.

FAO/IIASA/ISRIC/ISSCAS/JRC (2012), Harmonized World Soil Database (version 1.2), Food and Agriculture Organization of the United Nations, International Institute for Applied Systems Analysis, ISRIC - World Soil Information, Institute of Soil Science - Chinese Academy of Sciences, Joint Research Centre of the European Commission, Laxenburg

Gao, H., C. Birkett, and D.P. Lettenmaier. (2012), Global monitoring of large reservoir storage from satellite remote sensing. Water Resources Research, 48(9).

Gao, H. (2015), Satellite remote sensing of large lakes and reservoirs: From elevation and area to storage. *Wiley Interdisciplinary Reviews: Water*, 2(2), pp. 147-157.

Gebregiorgis, A.S. and F. Hossain (2014), Making Satellite Precipitation Data Work for the Developing World, *IEEE Magazine on Transactions in Geosciences and Remote Sensing*, June 2014 Issue, pp., 24-36 (doi: 10.1109/MGRS.2014.2317561).

Graf, W. L. (2006). Downstream hydrologic and geomorphic effects of large dams on American rivers. *Geomorphology*, *79*(3), pp. 336-360.

Keskinen, M. et al. (2012), Mekong at the crossroads: Next steps for impact assessment of large dams." *Ambio* 41(3), pp. 319.

M. Kummu, J. Sarkkula (2008), Impact of the Mekong river flow alteration on the Tonle Sap flood pulse Ambio, 37 (2008), pp. 185–192

Ji, Lei, L. Zhang, and B. Wylie. (2009), Analysis of dynamic thresholds for the normalized difference water index. Photogrammetric Engineering & Remote Sensing, 75(11), pp. 1307-1317.

Kummu, M., X.X. Lu, J.J. Wang, and O. Varis (2010). Basin-wide sediment trapping efficiency of emerging reservoirs along the Mekong.Geomorphology, 119(3), pp. 181-197.

Lehner, B., C.R. Liermann, C. Revenga, C. Vörösmarty, B. Fekete, P. Crouzet, and C. Nilsson, C. (2011), Global reservoir and dam (grand) database. *Technical Documentation, Version*, *1*.

Lehner, B., C.R. Liermann, C. Revenga, C. Vörösmarty, B. Fekete, P. Crouzet, & C. Nilsson. (2011), High-resolution mapping of the world's reservoirs and dams for sustainable river-flow management. Frontiers in Ecology and the Environment, 9(9), pp. 494-502.

Liang, X., D.P. Lettenmaier, E. F. Wood, S.J. Burges (1994), A simple hydrologically based model of land surface water and energy fluxes for general circulation models, Water Resour Res, 99(D7), pp. 14,415-14,428.

Ligon, F., W. Dietrich and W. Trush. (1995), Downstream Ecological Effects of Dams. BioScience, 45(3), pp. 183-192.

Lohmann, D., R. Nolte-Holube, and E. Raschke, (1996), A large-scale horizontal routing model to be coupled to land surface parametrization schemes, Tellus, 48(A), pp. 708-721.

Loveland, T. R., Reed, B. C., Brown, J. F., Ohlen, D. O., Zhu, Z., Yang, L. W. M. J., & Merchant, J. W. (2000), Development of a global land cover characteristics database and IGBP DISCover from 1 km AVHRR data. International Journal of Remote Sensing, 21(6-7), 1303-1330.

McGuire, Marketa, et al. (2006) Use of satellite data for streamflow and reservoir storage forecasts in the Snake River Basin. Journal of Water Resources Planning and Management, 132(2), pp. 97-110.

McFeeters, S. K. (1996). The use of the Normalized Difference Water Index (NDWI) in the delineation of open water features. International journal of remote sensing, 17(7), pp. 1425-1432.

Pringle, C. (2003). What is hydrologic connectivity and why is it ecologically important?. Hydrological Processes, 17(13), pp. 2685-2689, DOI: 10.1002/hyp.5145.

International Centre for Environmental Management, MRC Strategic Environmental Assessment (SEA) of Hydropower on the Mekong Mainstream (MRC, Hanoi, Vietnam, 2010); www.mrcmekong.org/ish/SEA.htm.

Rueda, F., E. Moreno-Ostos, and J. Armengol (2006). The residence time of river water in reservoirs. Ecological Modelling, 191(2), pp. 260-274.

Seeber, Christoph, Heike Hartmann, and Lorenz King. (2010). Land use change and causes in the Xiangxi catchment, Three Gorges Area derived from multispectral data. Journal of Earth Science 21(6). pp. 846-855.

Vörösmarty C.J , K.P. Sharma, B.M. Fekete , et al. (1997), The storage and aging of continental runoff in large reservoir systems of the world. Ambio, 26, pp. 210–19.

Zarfl, C., A.E. Lumsdon, J. Berlekamp, L. Tydecks, and K. Tockner (2015). A global boom in hydropower dam construction. Aquatic Sciences, 77(1), pp. 161-170.

7. Tables

Table 1: List of dams examined in this study and their capacities and degrees of regulation

Dam/Reservoir Name	Capacity [million m^3]	Degree of Regulation (%)
Haixihai	61.9	197.7
Zibihe	93.2	131.6
Manwan	920	3.2
Nam Ngum	7030	87.5
Nam Leuk	185	72.3
Nam Oun	520	70.4
Nong Han Lake	1873.9	155.6
Nam Pung	165.5	102
Ubol Ratana	2263	83.2
Lam Pao	1430	48
Chulabhorn	188	198.1
Huai Kum	22.8	15.7
Lam Chang Han	26	156.4
Lamtakhong	310	189.8
Lamphraphloeng	152	86.7
Lamnangrong	150	161.6
Pak Mun	229	0.7

Sirindhorn	1966	142.7
Houayho	596	395.6
Yali	1037	17.1

Table 2: Overall and seasonal residence time for each reservoir

Dam Name	Overall Residence Time (yr)	Dry Season Residence Time (yr)	Wet Season Residence Time (yr)
Haixihai	2.07	2.08	2.05
Zibihe	1.15	1.15	1.13
Manwan	0.12	0.18	0.07
Nam Ngum	1.16	1.18	1.15
Nam Leuk	0.58	0.59	0.45
Nam Oun	0.61	0.63	0.57
Nong Han Lake	2.33	2.35	2.32
Nam Pung	0.95	1.05	0.93
Ubol Ratana	0.56	0.61	0.50
Lam Pao	0.53	0.53	0.43
Chulabhorn	2.08	2.09	2.05
Huai Kum	0.22	0.30	0.21
Lam Chang Han	0.89	0.92	0.84
Lamtakhong	0.58	0.59	0.49

Lamphraphloeng	0.33	0.33	0.33
Lamnangrong	1.94	1.96	1.93
Pak Mun	0.09	0.25	0.06
Sirindhorn	0.96	1.04	0.91
Houayho	4.04	4.05	3.98
Yali	0.44	0.66	0.38

8. Figures

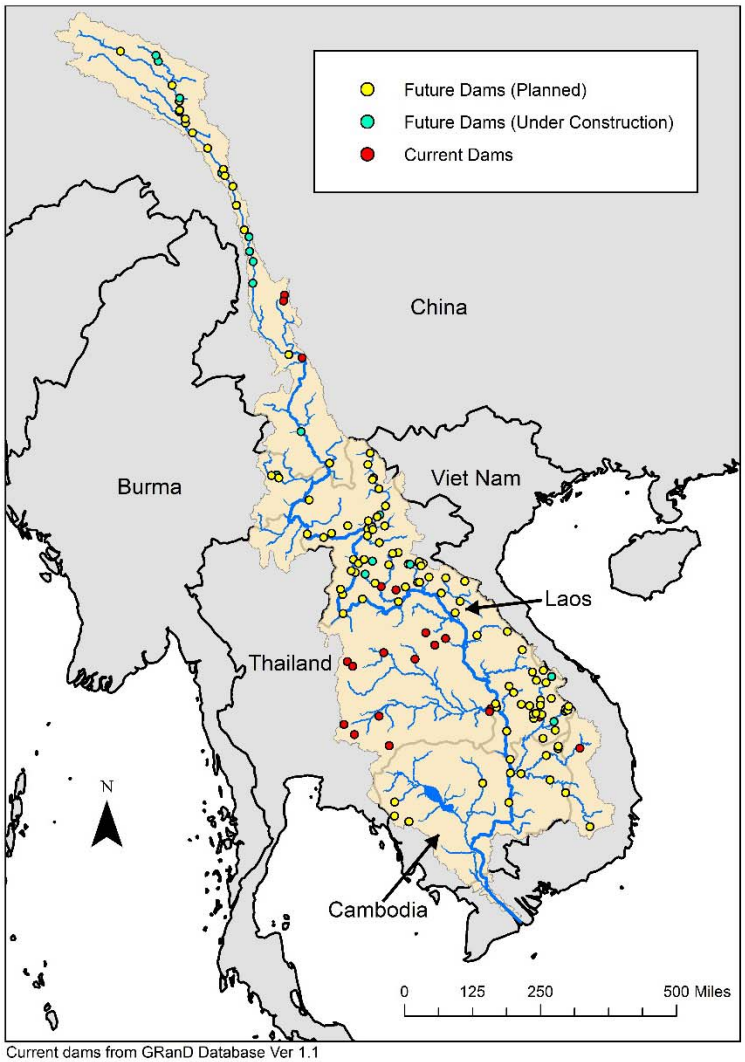

Current dams from GRanD Database Ver 1.1
Future Dams from Zarfl et al. 2015
River network and basin boundary from HydroSHEDS

Figure 1: Map of Mekong River Basin with current and future (planned) dams.

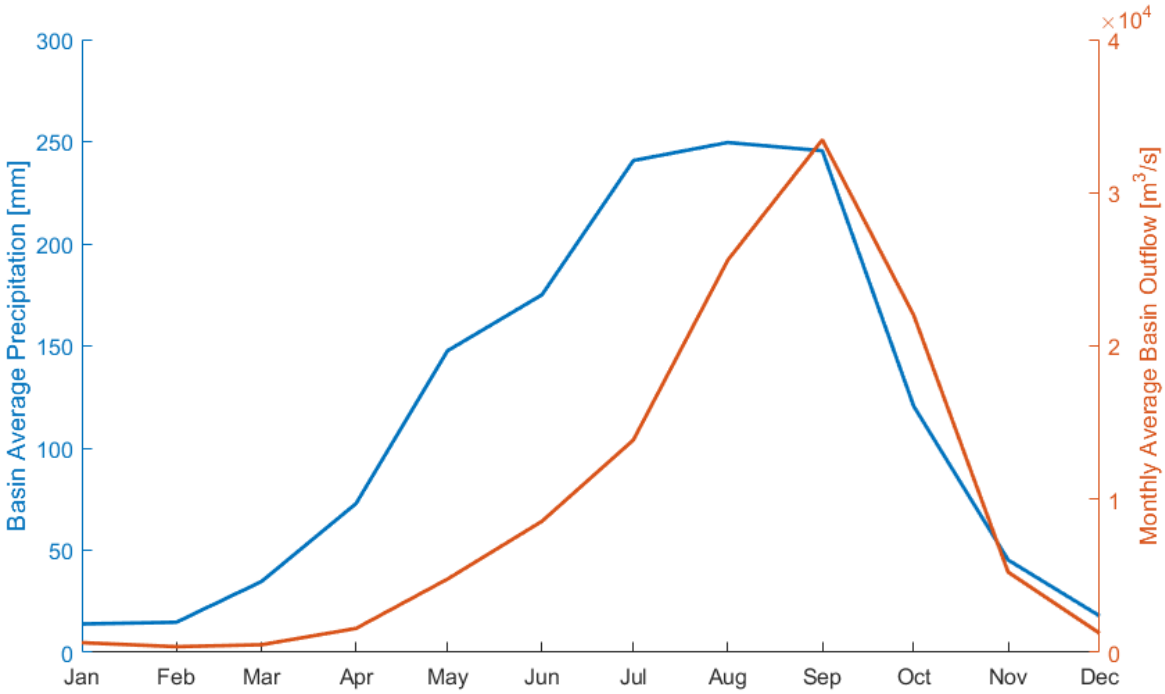

Figure 2: Monthly averaged basin precipitation and outflow at the MRB delta from VIC model.

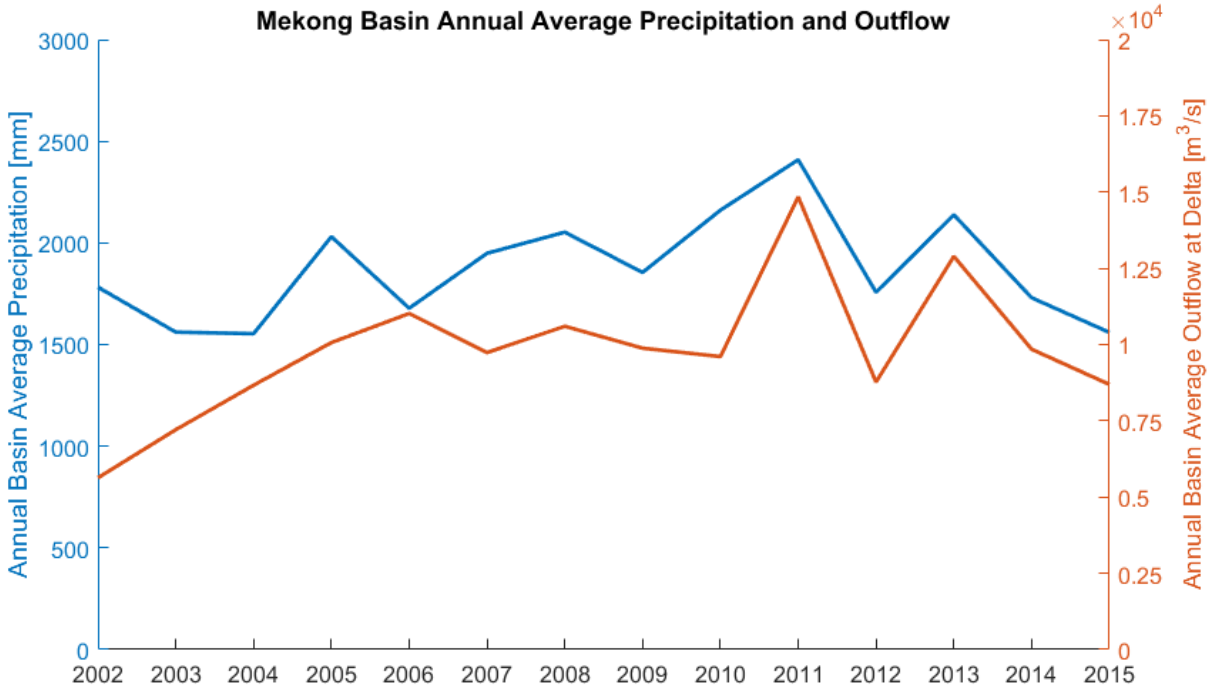

Figure 3: Average annual basin precipitation and outflow at delta from 2002 through 2015 from VIC model.

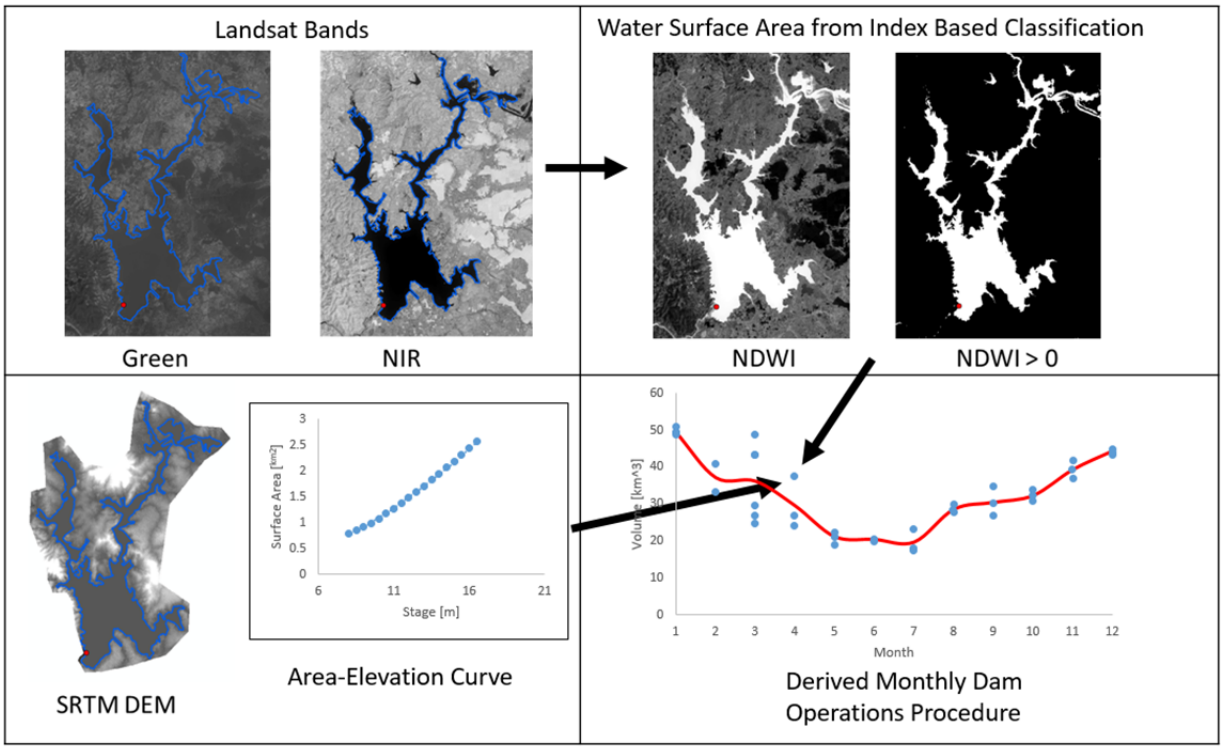

Figure 4: Flow chart depicting process of approximating reservoir operations curve. Upper left panel shows the green and NIR Landsat bands. Upper right panel shows the Normalized Difference Water Index (NDWI) and the classified water pixels. Lower left panel shows an area-elevation curve and the SRTM 30m DEM it was derived from. Lower right panel shows the operations curve. A single point on the curve is the result of the combination of one NDWI classified image with the area-elevation curve.

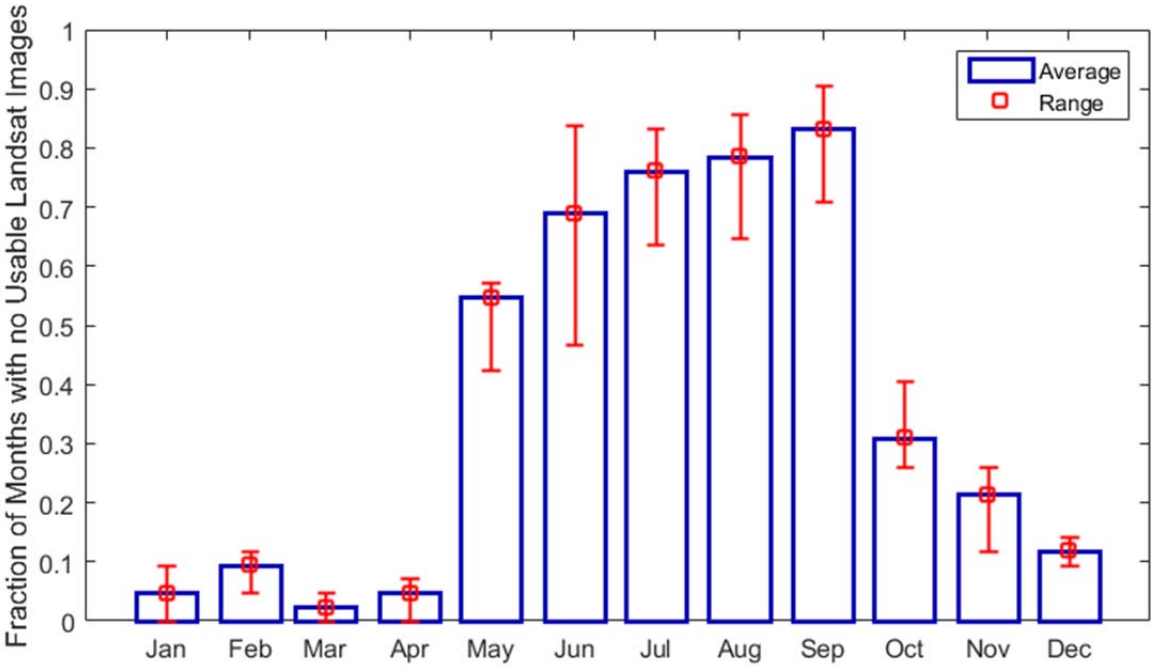

Figure 5: Average and range of fractions of months with usable Landsat observations, by month over the 14 year period.

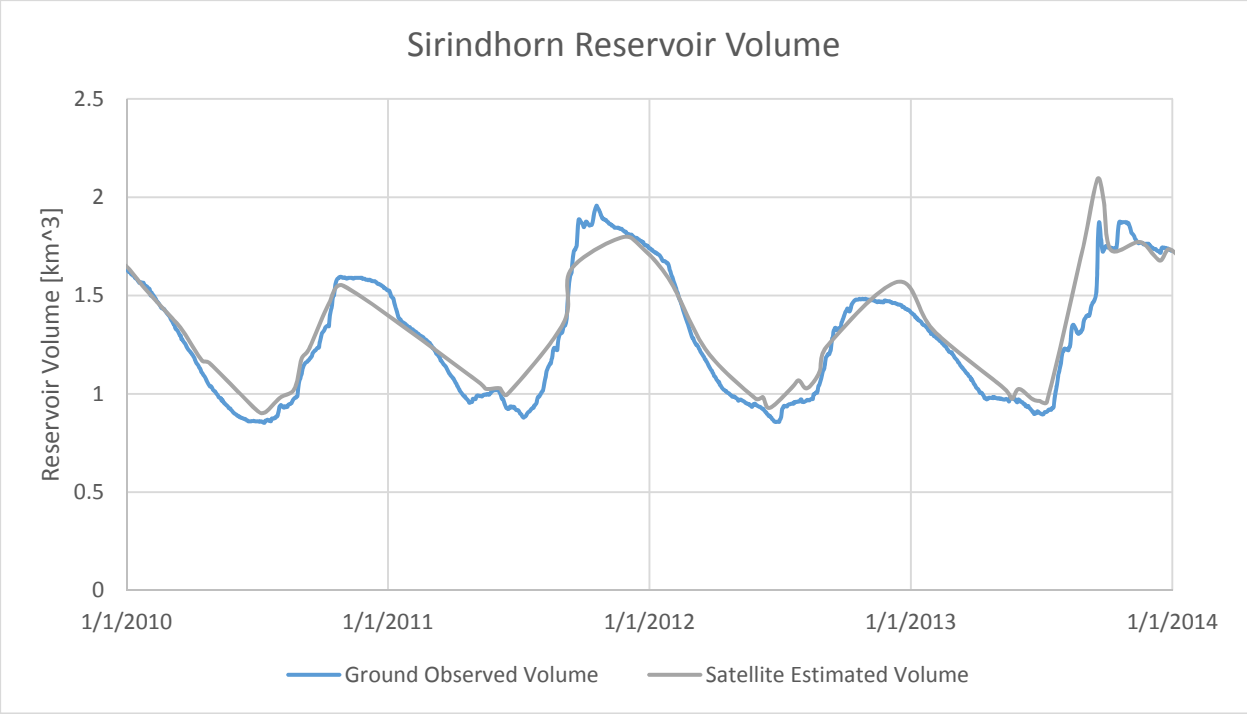

Figure 6: Comparison between ground observed and satellite estimated reservoir volume for the Sirindhorn Reservoir.

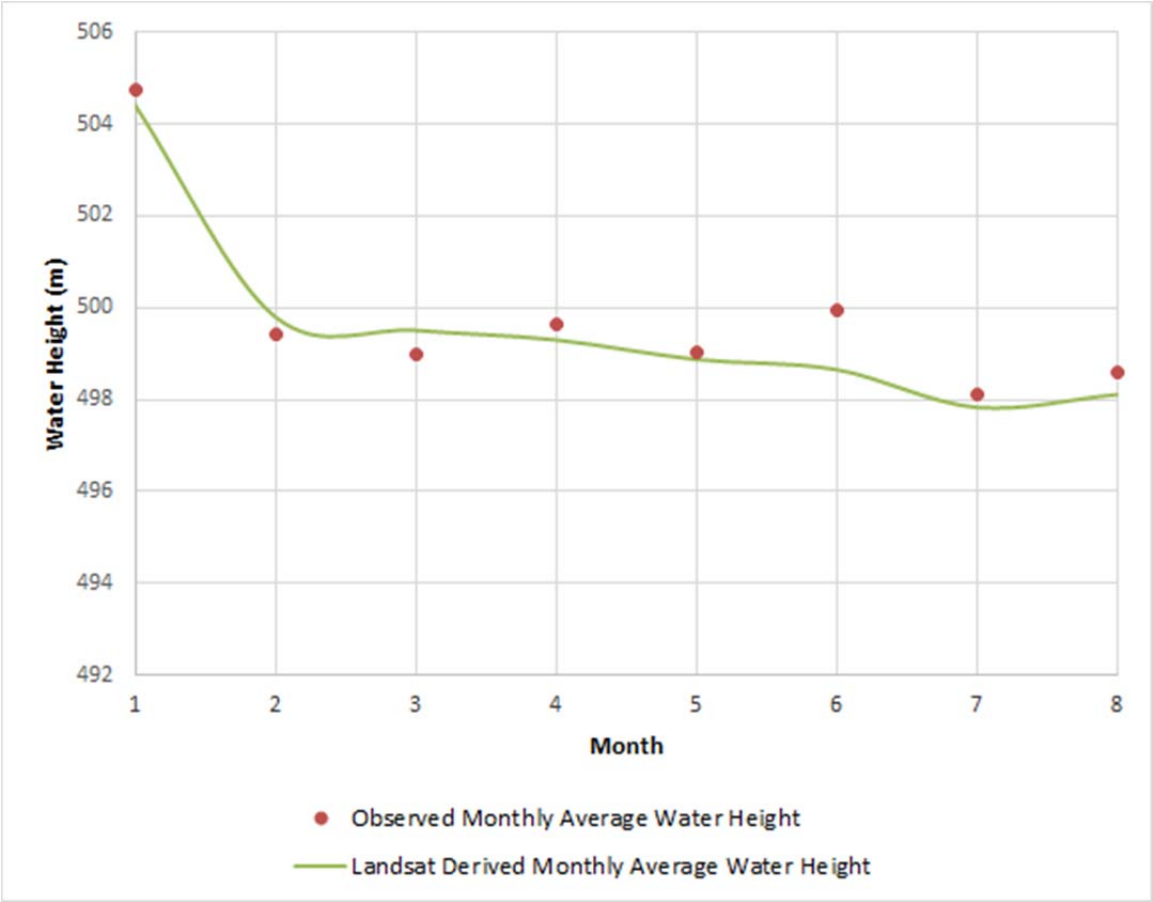

Figure 7: Comparison between observed monthly average water height and Landsat derived water height for the Yali Reservoir.

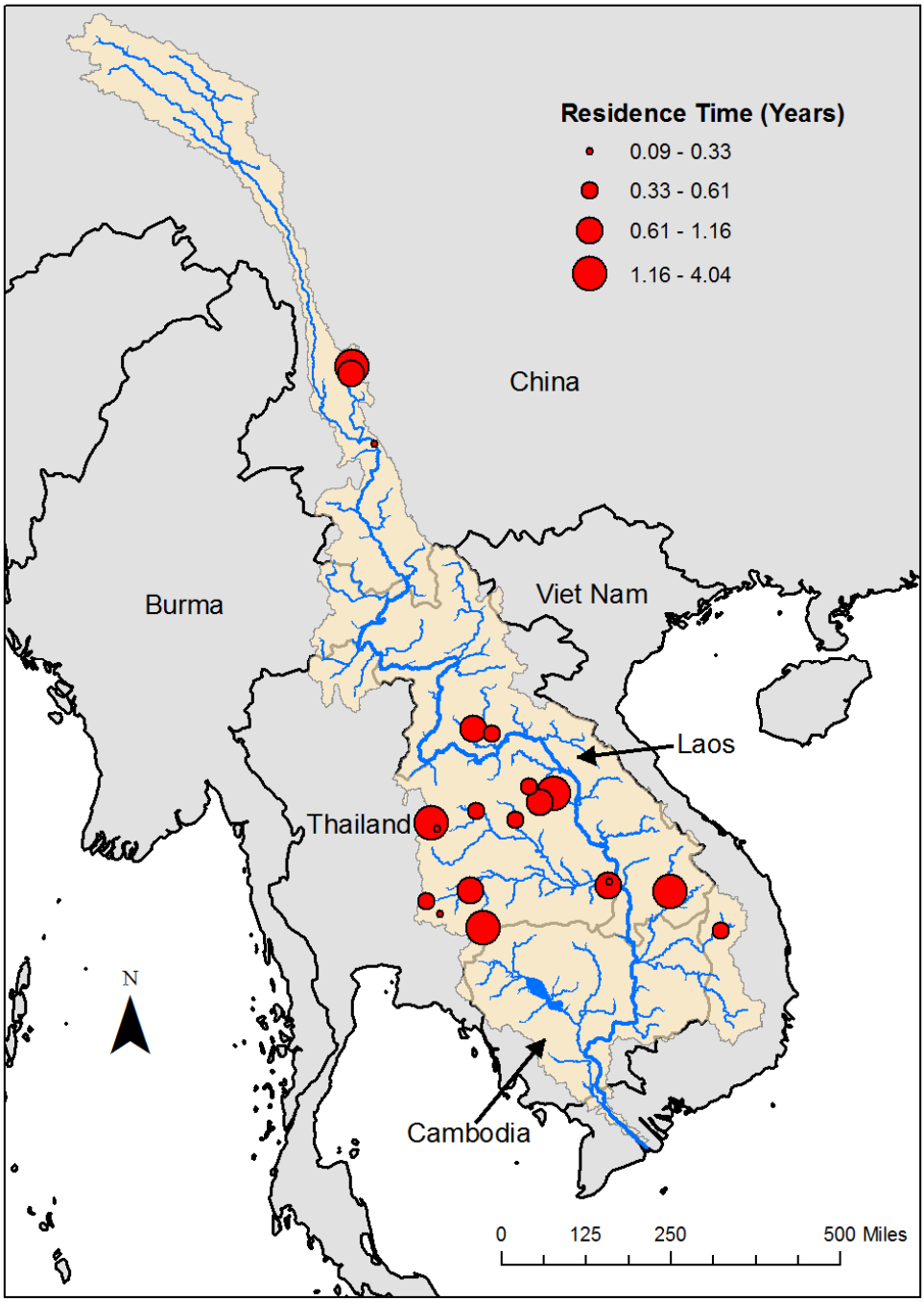

Figure 8: Map displaying the residence time of reservoirs in the Mekong Basin.

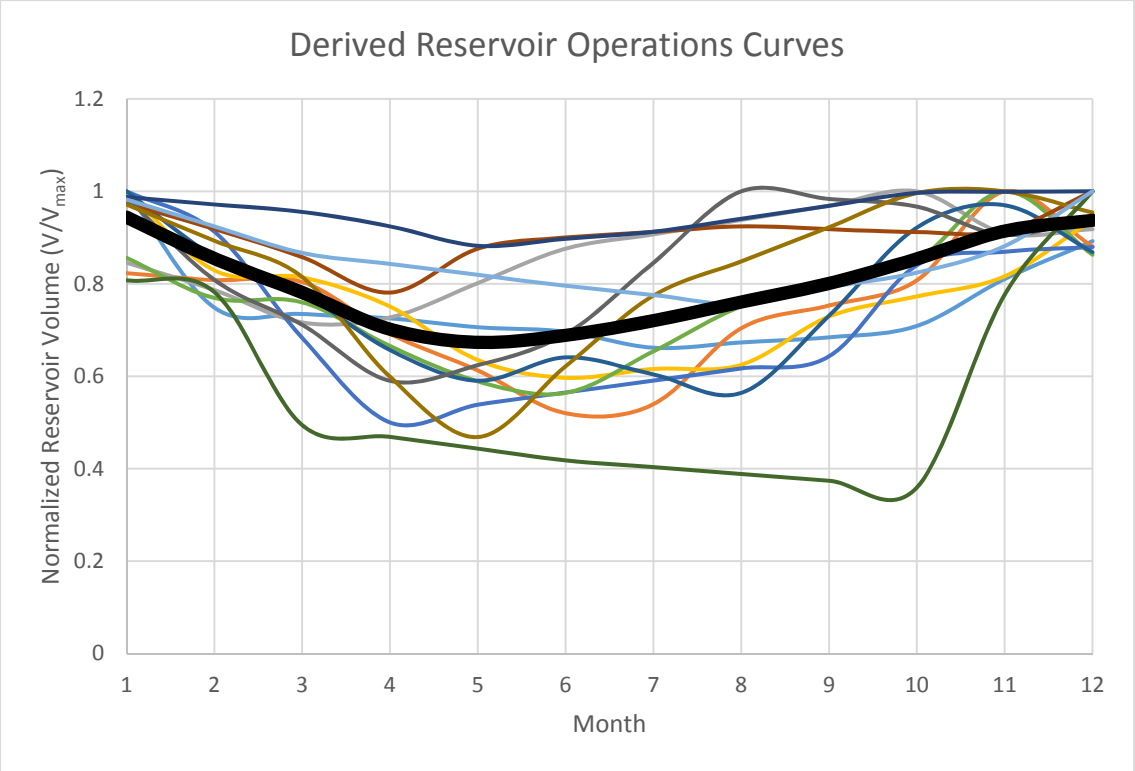

Figure 9: Derived reservoir operations curves (i.e. 'effective') for all reservoirs, normalized by reservoir maximum volume. Average shown in black.

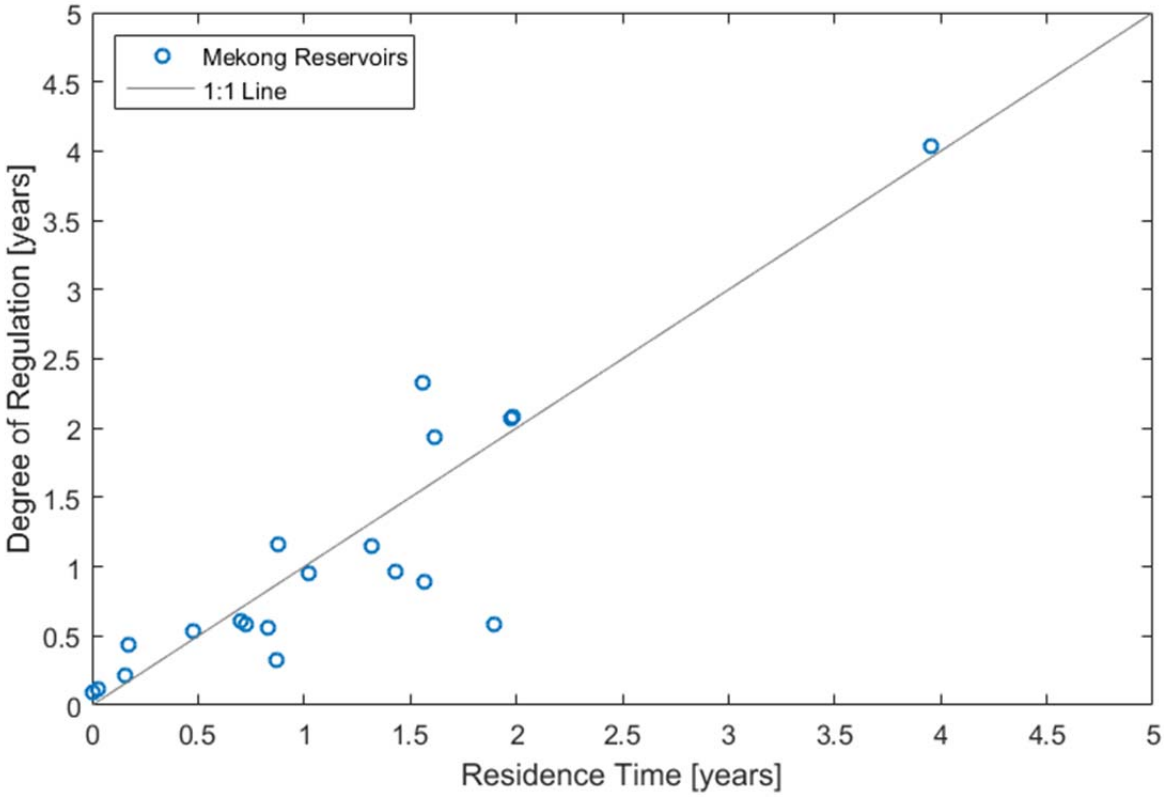

Figure 10: Comparison between residence time estimated in this study and degree of regulation (DOR) from the GRanD Database. Here, DOR is the reservoir capacity expressed in years of average annual inflow. 1:1 line shown in grey.

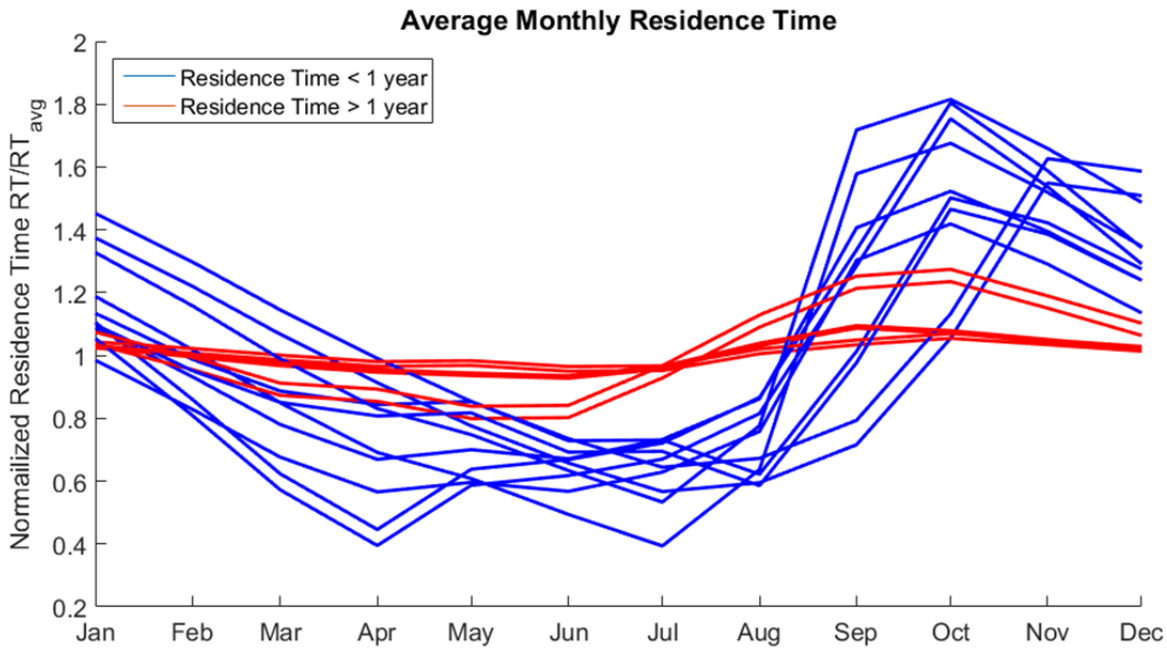

Figure 11: Average monthly residence time for each reservoir, normalized by each reservoir's average residence time. Reservoirs with residence time less than 1 year are shown in blue. Reservoirs with residence time greater than 1 year are shown in red.

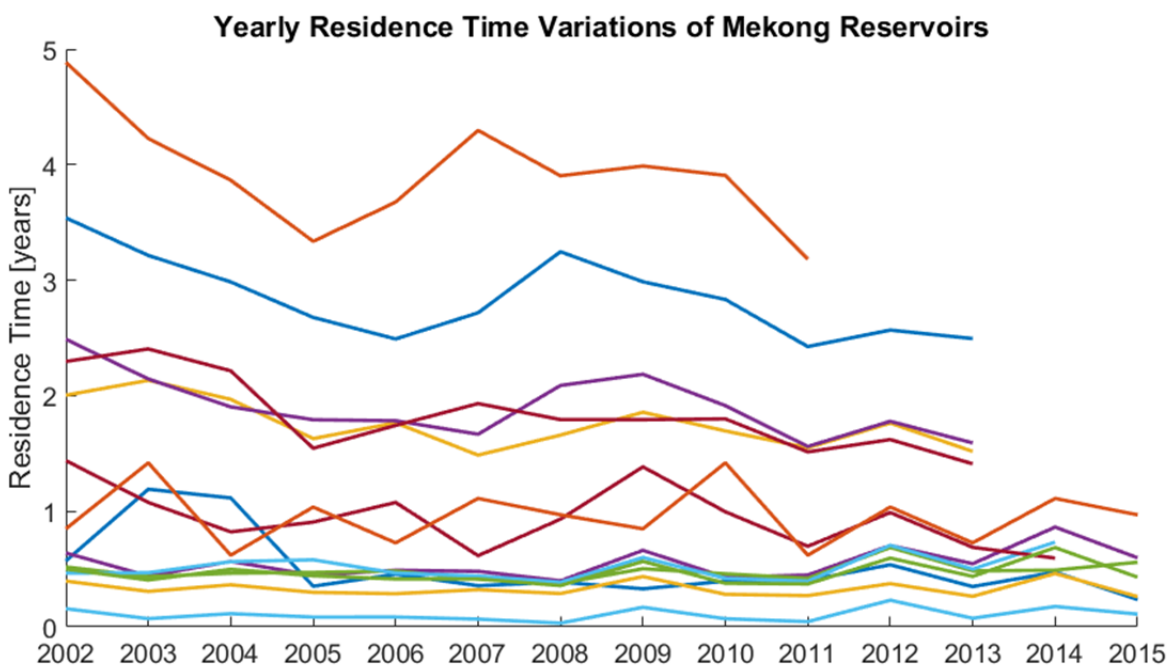

Figure 12: Residence time of each reservoir, averaged by year.

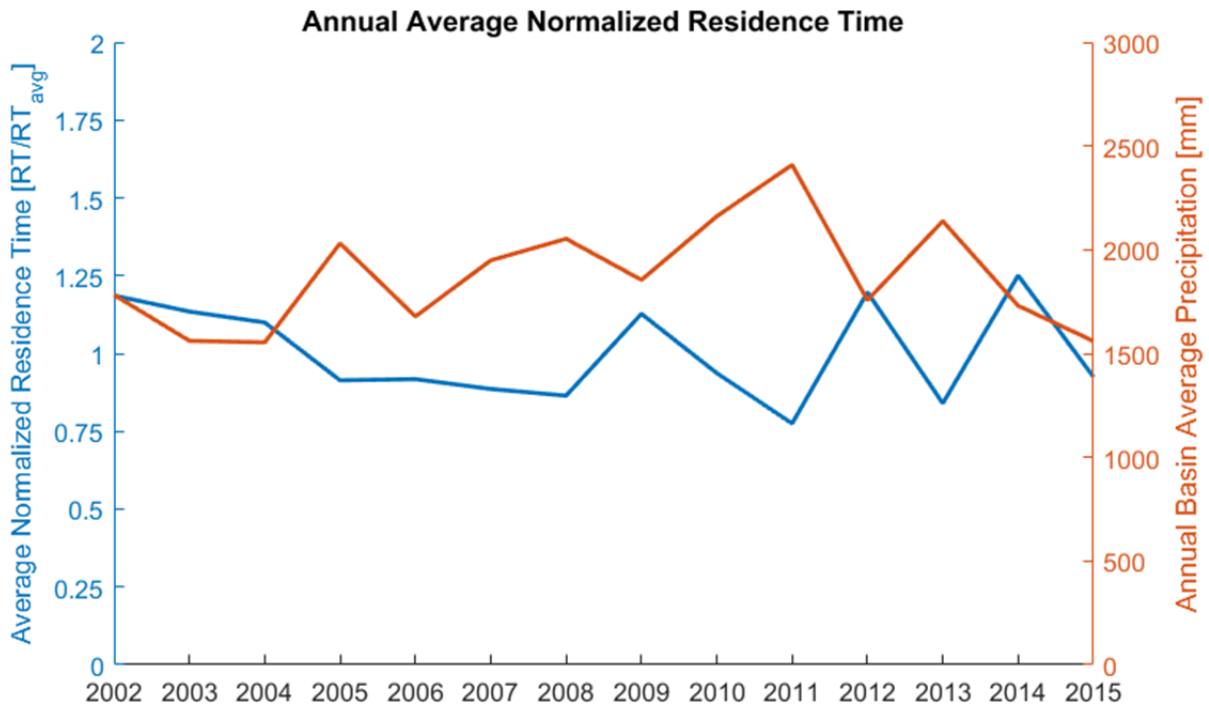

Figure 13: Basin average normalized residence time by year with average annual precipitation.

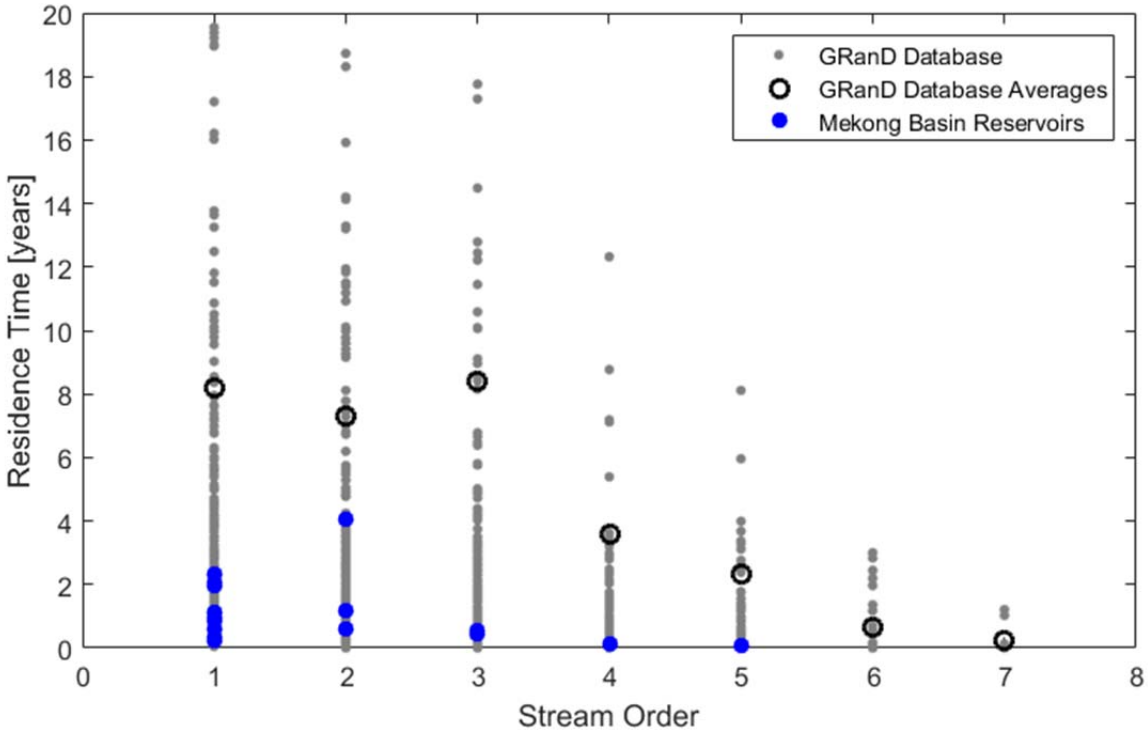

Figure 14: Stream order versus residence time for the MRB reservoirs as well as all GRanD Database reservoirs and their averages by stream order. GRanD Database residence time taken as the DOR expressed in years.